

# DEFENCE RESEARCH ESTABLISHMENT OTTAWA

DEFENCE RESEARCH BOARD OF CANADA

## OPERATION DIAL PACK 1970 CANADIAN PROJECT A7 THERMAL RADIATION MEASUREMENTS

by

J.D.R. Pattman



REPORT NO. DREO 642

PROJECT NO.  
DRB 16-01-39

12  
AUGUST 1971  
OTTAWA

**DEFENCE RESEARCH BOARD**

**DEPARTMENT OF NATIONAL DEFENCE  
CANADA**

**DEFENCE RESEARCH ESTABLISHMENT OTTAWA**

**REPORT NO. DREO 642**

**OPERATION DIAL PACK 1970 — CANADIAN PROJECT A7  
THERMAL RADIATION MEASUREMENTS**

by

J.D.R. Pattman

Radiation Measurements Section  
NBC Defence Division

**Project No. DRB 16-01-39**

**August 1971  
OTTAWA**

(i)

Operation DIAL PACK 1970 - Canadian Project A7  
Thermal Radiation Measurements

ABSTRACT

Thermal radiation from the DIAL PACK 500-ton TNT explosion was recorded in selected wavelength bands, using a high-speed bolometer system, photo-electric detectors, and calorimeters. The radiation was received in both broad and narrow spectral bands, defined by placing suitable combinations of glass filters and silica windows in front of the detectors.

Results were obtained from all instruments used, and are presented in this report. These include measurements of the total thermal energy radiated, the thermal pulse shape as shown by records of irradiance versus time, and the variation of spectral distribution as a function of time. Estimation of the apparent temperature of the fireball surface is also discussed.

Some comparisons are made with results from previous large TNT explosions.

Opération DIAL PACK 1970 - Projet Canadien A7  
les mesures de rayonnement thermique

RÉSUMÉ

La chaleur de l'explosion de 500 tonnes de TNT (opération DIAL PACK), a été enregistrée en longueur d'ondes choisies à l'avance, avec un système de bolomètre rapide, des détecteurs photo-électriques, et des calorimètres. Le rayonnement était reçu par les détecteurs en bandes spectrales larges et étroites. Des filtres en verre et en silice placés en avant des détecteurs déterminaient les longueurs d'ondes.

Les instruments utilisés fonctionnaient l'une façon satisfaisante et tous les canaux ont donné des résultats. Ces résultats comprennent les mesures de l'énergie thermique totale, la forme de l'impulsion thermique telle que montrée par les enregistrements de l'histoire du flux lumineux, et les variations de la distribution spectrale en fonction du temps.

Une discussion de la température apparente de la surface de balle de feu est incluse.

Enfin, nous avons fait certaines comparaisons avec des explosions de TNT observées précédemment.

## 1. INTRODUCTION

DIAL PACK was the code name given to a field trial carried out at the Watching Hill test range of the Defence Research Establishment Suffield on 23 July, 1970. The trial was based upon the explosion of a 500-Ton TNT charge, built from rectangular blocks each weighing 32.6 pounds arranged in a form approximating a sphere tangential to the ground. The lower half of the sphere was supported by styrofoam and the whole charge was placed upon a plywood base. Figure 1 shows the charge design, and Figure 2 is a photograph of a similar charge used during a previous trial. Detonation was initiated at the center of the charge at 1100 hrs MST. The projects associated with this trial included basic blast measurements and the assessment of blast effects. Included in the early-time phenomenology studies was a project designed to measure the thermal radiation from the explosion. The project was designated Canadian Project A7, Thermal Radiation Measurements, and this report is concerned with various aspects of this project.

Objectives included the measurement of radiation in both narrow and wide spectral bands to examine the thermal pulse shape, to calculate the total thermal yield, and to estimate the temperature of the fireball surface. Other projects associated with the DIAL PACK operation are outlined in Suffield Memoranda 16/70 and 57/70 (1, 2).

## 2. METHOD

The irradiance from the explosion was measured in selected wavelength bands, and recorded as a function of time. Suitable corrections were applied to compensate for atmospheric absorption, and values of radiant intensity were obtained by using the inverse-square law. Combining these values with the apparent area of the fireball as seen from the instrument sites, it was then possible to compute the radiant emittance.

The thermal pulse-shape was found by plotting the values of radiant intensity against time. Integration of this curve with respect to time, gave a figure for the total thermal yield from the explosion. Total thermal yield was also measured by means of self-integrating thermo-electric calorimeters.

Comparison of the radiant emittance measurements in selected wavelength bands with the theoretical values for a black-body emitter, provided an indication of the fireball temperatures. Temperatures were also estimated by taking ratios of radiant intensities measured in pairs of spectral bands, and

comparing these with ratios calculated for a black-body emitter. In this text, temperatures inferred from radiant emittance measurements in single spectral bands and using the apparent area of the fireball, are referred to as emittance temperatures, and denoted by the symbol  $T_E$ . Those temperatures obtained from ratios of radiant intensities, are referred to as distribution temperatures, and denoted by the symbol  $T_D$ . Values for  $T_D$  and  $T_E$  may not be the same at any given time, and in fact will not be the same unless the fireball emits as a black-body. Further details concerning the methods used to analyze the records will be found in DASIAC Special Report SR 60 (3).

### 3. INSTRUMENTATION

Three types of instruments were used to measure the thermal radiation from the explosion. High-speed bolometers receiving radiation in broad spectral bands defined by coloured glass filters and/or fused silica, recorded the radiant power on galvanometer-type oscillographs. Vacuum-photocell detectors were used to measure the radiation in narrow wavelength bands defined by glass filters. The photocell records were displayed on a cathode-ray oscilloscope and photographed with a Polaroid camera. Finally, thermo-electric calorimeters were used to measure the total radiant energy from the explosion.

Wavelength bands of the bolometer system are referred to by the designation of the filtering material. The detectors had fused silica windows which defined the overall spectral limits of the system, and Chance OY4 (yellow), or OX2 (infra-red) glass was added where required. The vacuum-photocell system had six channels numbered 1 (U.V.), 2 (blue), 3 (green), 4 (red), 5 (infra-red) and 6 (infra-red). The pass bands of the filters used with the bolometer and photocell systems are shown in Fig. 3.

The instrument systems are described in more detail elsewhere (4, 5, 6). Characteristics of the instruments used for this trial, and siting arrangements are given in Table I.

Calibrations of the instruments were carried out both in the laboratory and in the field, using suitable sources of known spectral distribution (such as the sun, and standard incandescent lamps) monitored with a calibrated wide-band thermopile. Details of calibration methods are given in an appendix to DCBRL Report No. 488 (7).

### 4. UNITS AND SYMBOLS

Radiometric units are used in this report, and as far as possible nomenclature of ASA Standard Z58.1.1-1953 is followed, (8). The calorie is selected as a basic unit of energy, and the other units and symbols are given in the table below.

Radiometric Quantity	Symbol	Units	
Irradiance	H	cal cm <sup>-2</sup> s <sup>-1</sup>	
Radiant density	u	cal cm <sup>-2</sup>	u = ∫H dt
Radiant energy	U	cal	U = 4πr <sup>2</sup> u
Radiant intensity	J	cal s <sup>-1</sup> ster <sup>-1</sup>	J = Hr <sup>2</sup>
Radiant emittance	W	cal cm <sup>-2</sup> s <sup>-1</sup>	W = J π/A

In addition we refer to the radiometric quantities normalized to unit spectral-band width. These quantities are distinguished by the subscript  $\lambda$ . Thus spectral radiant emittance has the symbol  $W_\lambda$ , and is given in units of cal cm<sup>-2</sup> s<sup>-1</sup> nm<sup>-1</sup>.

The following general symbols or abbreviations are used in the above table:

- A - apparent area of fireball, as seen from instrument site, (cm<sup>2</sup>).
- nm - nanometre (1 x 10<sup>-9</sup> metre).
- r - range, from ground zero to instrument site, (cm).
- ster - steradian, unit solid angle.

## 5. RESULTS

Records were obtained on all channels of instrumentation used, and the most useful records were analysed. Other records, where low signal-to-noise ratio limited their usefulness, were examined in less detail to substantiate the overall analysis. The results have been tabulated in this report. In some cases graphical display has also been used.

### BOLOMETER RESULTS

Table II shows results of bolometer measurements. Columns 2, 3, and 4, show results from three broad spectral bands, designated silica, OY4 and OX2. The silica band had only the silica window in front of the detectors, the OY4 band had in addition a 4-mm-thick Chance OY4 glass filter and the OX2 band had a 4-mm-thick Chance OX2 glass filter in front of the silica window. Spectral details of these channels are shown in Table I and also in Fig. 3. Low accuracy of measurements in the OY4 and OX2 bands at early times does not justify their inclusion here. It will be noted that

the transmission factor,  $a$ , shown in column 7 of Table II, varies with time.

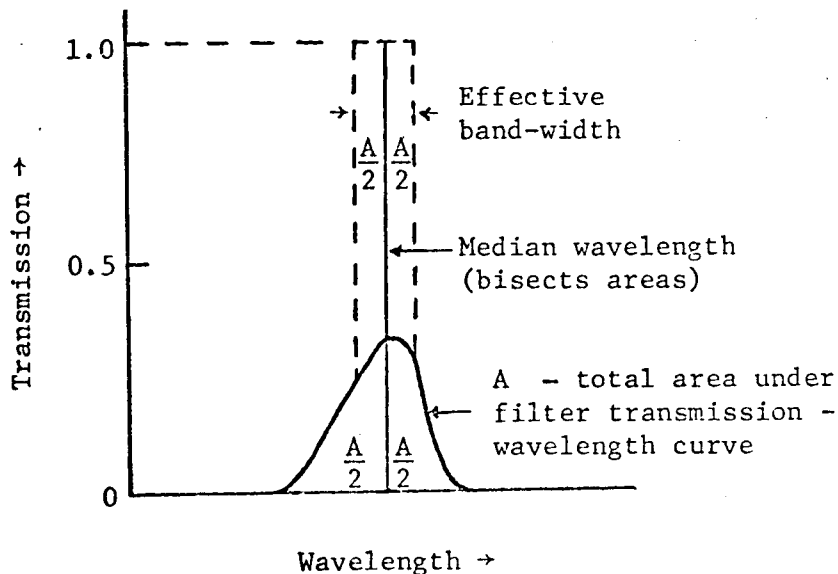
Two factors contribute to this variation, both related to absorption due to water vapour in the atmosphere. This absorption takes place in relatively broad bands in the infra-red region. The first factor which affects the apparent atmospheric transmission results from a drop in temperature of the fireball surface, and the consequent shift in spectral distribution of the emitted radiation. As the fireball cools, the peak radiant emittance shifts towards the infra-red, and thus an increasingly large part of the total radiant emittance appears in this region. The apparent effect is a decrease in the transmission of the broad-band radiation from the fireball, since the absorption due to water vapour occurs in this spectral region. The second factor producing a variation in the transmission, results from the rise of the fireball into air of lower humidity. This results in an increase in the apparent transmission of the atmosphere, but in the present case, this second and opposite effect on the transmission, was smaller than the effect due to the decrease in temperature of the fireball surface. Both effects were considered and combined to give the values for the atmospheric transmission factors,  $a$ , shown in Table II, column 7.

The results in the last column, radiant intensity, are plotted with respect to time in Fig. 4, showing the thermal pulse shape.

#### PHOTOCELL RESULTS

Table III (a) shows the photocoell results, with steps leading to the estimation of the distribution temperatures for the fireball surface. The values of spectral irradiance given in columns 8 to 13 were found by dividing the respective values of irradiance measured at site by the effective band-width of the system in each channel. This was done in order to compare irradiances in various parts of the spectrum, in terms of unit band-width. We define the effective band-width as the width of an ideal band-pass filter having a transmission factor of 1.0 (100%), which has the same transmission band-width product as the filter in question.

This is illustrated below, in simplified graphical form.



The values of effective band-width used for these calculations are given in Table I.

Table III (b) shows the photocell results also, with the steps used to estimate values of emittance temperature,  $T_E$ . The figures given in column 2 for apparent fireball area were obtained by measuring areas displayed on selected frames from a moving film record of the explosion. The framing speed of the camera, with time intervals between frames of 0.225 milliseconds, was not fast enough to give high accuracy at the earliest times shown. This may be a factor in the variation of values for  $T_E$ , at times prior to one millisecond, and may also account for the minimum in the emittance temperature versus time relationship displayed in this table at 0.94 milliseconds. It is thought that this minimum is not a real effect.

The values for distribution temperature,  $T_D$ , shown in the last two columns of Table III (a), were obtained by reading temperatures from the relevant curve in Fig. 5 for the respective values of irradiance ratios. Irradiance values are given in columns 2 to 7, and the ratios used are shown in the headings for the last two columns. Similarly, the values of  $T_E$  given in columns 9 to 12 of Table III (b) were taken from calibration curves shown in Fig. 6. These calibration curves, together with those in Fig. 7 were prepared from theoretical radiation tables of Lowan and Blanch (9).

Fig. 8 shows curves of temperature-time functions prepared from the data in Tables III (a) and III (b). Only three curves are shown here in order to clarify the presentation. The relatively wide variations in temperature at early times, and the good agreement at times after about 10 milliseconds are clearly seen.

#### CALORIMETER RESULTS

Results obtained from the thermo-electric calorimeters are displayed in Table V. It will be seen that reasonable agreement was shown between five of the six channels used. Results from calorimeter 10-1 are unrealistically low, and values from this channel were not included in averages shown elsewhere. A single value for the transmission factor was used for each of the two sites where calorimeters were exposed. This was justified because the majority of the radiation received by the calorimeters was emitted by the fireball while it was a relatively constant temperature. This may be seen by inspecting Table II, column 7, which shows the transmission factor,  $a$ , to lie between 0.58 and 0.55 for the period from 0.1 second to 15 seconds. The transmission factors used in conjunction with the calorimeter results are shown at the bottom of Table V.

It was found useful to refer to Suffield Technical Note No. 114 on transmission (10) to make corrections for atmospheric absorption.



## 6. DISCUSSION

## THERMAL PULSE SHAPE

Examination of the thermal pulse shown in Fig. 4, reveals the familiar maxima and minima displayed by thermal pulses from previously observed explosions. The maximum at about 325 ms is particularly prominent in this pulse. This maximum is generally referred to as the "second shock brightening", produced by increased chemical activity as the second (reflected) shockwave passes through the flame front. Rudlin (11) has recently referred to this second shock as the Wrecker shock. The subsequent maxima may be brightenings resulting from the passage of further reflected shock waves, but we have no additional evidence to support this.

The thermal pulse is shown in dimensionless form in Fig. 9, together with pulses from the 100-Ton, 1961 explosion, and the 500-Ton 1964 explosion. It will be seen that although there is a general resemblance between the curves, the various features are not closely scaled, either with respect to time or with respect to intensity. An unexpected feature of the DIAL PACK pulse, was the late appearance of the first light emitted from the charge. Previous measurements by our group have shown relatively close scaling for the time to first light. We have allowed 0.024 ms for the function time of the detonator in each case. The times to first light from the receipt of a pulse from the firing line, corrected for delay in start of detonation, are shown in the table below.

TIMES TO FIRST LIGHT

	Charge Radius  r	  r/r <sub>100</sub>	Time to First Light  t	  t/t <sub>100</sub>	t <sub>calc</sub> =  r x $\frac{t_{100}}{r_{100}}$	  t/t <sub>calc</sub>
1961, 100-ton Hemi-sphere	9.9 ft	1.00	0.46 ms	1.00	0.46 ms	1.00
1964, 500-ton Hemi-sphere	17 ft	1.72	0.78 ms	1.69	0.79 ms	0.99
1966, 20-ton Sphere	4.6 ft	0.465	0.23 ms	0.50	0.21 <sub>4</sub> ms	1.07
1970, 500-ton Sphere	13.5 ft	1.36	0.77 ms	1.68	0.63 ms	1.23

We have arbitrarily taken our first measurement (1961) as a standard and compared subsequent results with this standard.

It will be seen from the last column that close agreement between calculated and measured times to first light were observed in 1961 and 1964, and the value of 1.07 given for  $t/t_{\text{calc}}$ , 1966, is in fair agreement considering the reduced time scale and consequent faster time resolution required for the shorter pulse. The 1970 value for  $t/t_{\text{calc}}$ , (1.23) seems to indicate reduced velocity of the detonation front through the solid TNT, or much longer functioning time for the detonator.

A test was made to see if better scaling of the thermal pulses shown in Fig. 9 would result from the use of the calculated value, (0.63 ms), for the time  $t_1$ , (time to first light), in scaling values for the DIAL PACK thermal pulse curve. However, no overall increase in agreement with the other curves was apparent.

From measurements made to date by this group, it appears that close scaling of relative times and intensities for the thermal pulse is not possible.

#### SPECTRAL DISTRIBUTION

Two photocell channels not used in previous trials were included for DIAL PACK. Channel 1 used filters providing a narrow pass-band in the ultra-violet region, and channel 4 transmitted a narrow band in the red part of the visible spectrum. Further details of the filter characteristics are given in Fig. 3 and in Table I.

Fig. 10 shows the spectral distribution of the radiation from the explosion as measured by the photocell system, displayed as a function of time. It can be seen that peak irradiances occurred, first in the ultra-violet, then consecutively in the blue, green, red, and infra-red. The same information is displayed in Fig. 11 in a different manner. Here we have drawn a family of smooth curves, in each case joining values of spectral irradiance measured by the six photocell channels at one time. Times for each curve were selected to display graphically the shift to longer wavelength of the peak irradiance, at succeeding times. If we assume that the radiation is emitted by a black-body we can apply Wien's wavelength-temperature displacement law to the peaks shown by these curves, and infer temperature of the fireball surface from the results. Wien's law may be stated in the following form,

$$\lambda_{\text{max}} T = \text{constant}$$

where the constant is 0.289 cm °K.

Estimates of temperature were made in this manner and are shown in Table IV. Comparison of these temperature results with those in Tables II and III (a) (or with the curves shown in Fig. 8) give a clear indication of the difficulty of estimating the fireball temperature at times close to the first intensity maximum of the thermal pulse. It will also be noted that at times later than about 10 ms, there is substantial agreement between most of the temperatures derived by the various methods. The reason for the discrepancies

undoubtedly lies in assuming that black-body radiation theory can be applied to radiation from TNT explosions.

The high-resolution spectrographic measurements of thermal radiation from TNT explosions made by the group from Denver Research Institute (12), and also records from the Snow Ball explosion in 1964, contain evidence of considerable structure, identifiable as radiating species. From all the evidence one must conclude that black-body radiation theory does not fit the fireball at early times, and it is difficult or impracticable to estimate temperature by optical methods during this period in the fireball history.

#### THERMAL YIELD

Calorimeter results provided a value for the total thermal yield from the explosion. Thermal yield was also found by integrating bolometer measurements of radiant intensity with respect to time. From the average of calorimeter and bolometer results, a curve describing the history of the thermal yield was prepared, and is shown in Fig. 12.

It has been our practice to express the total thermal yield as a percentage of the blast yield, a custom dating from early nuclear explosion measurements, where partition of energy was considered important. The theoretical blast yield of TNT is taken to be  $1.0 \times 10^9$  calories per ton.

Thus the total theoretical blast yield for the DIAL PACK explosion was  $500 \times 10^9 = 5 \times 10^{11}$  calories.

The total thermal yield measured by the calorimeters at 600 metres range was  $3.5 \times 10^{10}$  calories.

Calorimeter results and bolometer results at 1,700 metres range gave a figure of  $3.7 \times 10^{10}$  calories. These figures are shown in Table VI, and are also expressed as percentages of the blast yield in the last column of this table.

It should be pointed out that the bulk of the thermal radiation recorded by our instruments was emitted at relatively late times, (see Fig. 12) when it could have little or no effect upon, or be affected by the blast wave. In fact most of the radiation comes from hot gases and carbon particles which are residual from the initial rapid chemical reaction which produces detonation. For this reason, it might be more logical to give the thermal yield as a percentage of the calculated heat of combustion for the charge. Heat of combustion for TNT is approximately  $3.3 \times 10^9$  calories per ton and on this basis the thermal yield for DIAL PACK can be given as 2.2% of the calculated heat of combustion for the charge.

#### 7. CONCLUSIONS

The first appearance of thermal radiation at the surface of the charge was later than predicted by scaling from previous TNT explosions

measured in a similar manner by this group. This may have been due to a delay in initiating the detonation or slower detonation velocity through the charge or both.

In general the thermal pulse displayed the expected features including the initial fast rise in radiant intensity followed by a large minimum and a second, main, maximum. Second shock brightening was very prominent, and further, smaller brightenings were seen. Scaling factors applied to the thermal pulse did not produce any close resemblance to other pulses measured previously, and it is concluded that it is not possible to accurately predict times or intensities of the various features by this means.

The presence of ultra-violet radiation of relatively high intensity was observed at early times. This is the first time that we have used a detector capable of measuring radiation in this portion of the spectrum, and have no reason to believe that ultra-violet radiation was not present in previous explosions.

The estimation of surface temperatures at early times was again shown to be difficult, or perhaps unrealistic, using the optical methods described here. At later times, after 10 milliseconds, fair agreement between the various temperature measurements described was evident. Unfortunately, the earlier times would be of more general interest, as it is during this period that the flame front is close to the shock front. The conclusion to be drawn from the temperature measurements, is that the fireball does not emit as a black-body radiator, and estimates based on black-body radiation theory are not valid.

The total thermal yield expressed as a percentage of the theoretical blast yield, (7.2%) was close to the average value obtained from the majority of previous similar experiments.

## 8. ACKNOWLEDGEMENT

The author wishes to acknowledge the fine support provided by the staff of DRES in the field, and in particular the technical assistance of Mr. F.L. McCallum provided throughout the trial.

## 9. REFERENCES

1. Watson, J.S., Hart, W.D., et al. "Event DIAL PACK". Suffield Memorandum 16/70 July 1970.
2. Wyld, R.C., Smart, G.P. "Canadian Participation in Event DIAL PACK" (F.E. 594). Suffield Memorandum No. 57/70 Nov. 1970.
3. Pattman, J.D.R., "Thermal Radiation and Fireball Temperatures, Operation Distant Plain, 1966", DASIAC Special Report SR 60.
4. Carruthers, J.A. and Pattman, J.D.R., "Bolometer System for Thermal Measurements", DRCL Report No. 263 (1957).
5. Dahlstrom, C.E. and Cunningham, J.R., "Radiometers and Calorimeters for Thermal Measurements", DRCL Report No. 264 (1957).
6. Tate, P.A. and Pattman, J.D.R., "Surface Burst of 100-Ton TNT Hemispherical Charge (1961), Project No. 4, Thermal Measurements", DRCL Report No. 371 (1962).
7. Pattman, J.D.R., and Tate, P.A., "Surface Burst of 500-Ton TNT Hemispherical Charge (1964) Project No. 4, Thermal Measurements", DCBRL Report No. 488 (1966).
8. American Standards Association Sectional Committee Z-58. "American Standards Association Nomenclature for Radiometry and Photometry, Z-58.1.1.-1953", Journal of the Optical Society of America, 43, 809 (1953).
9. Lowan, A.N. and Blanch, G., "Tables of Planck's Radiation and Photon Functions", Journal of the Optical Society of America, 30, 70, (1940).
10. McCallum, F.L. and Muirhead, J.C., "Transmission of the Atmosphere in the 0.325 to 4.6 micron (Silica) Band", Suffield Technical Note No. 114 (1963).
11. Rudlin, L., "On the Origin of Shockwaves from Condensed Explosions in Air", U.S. NOL Report, NOLTR 69-74, (1970).
12. Wisotski, J., "Early Explosion Phenomena from Operation Distant Plain", University of Denver, Denver Research Institute, Report 3884-6801-F (1968).

## LIST OF TABLES

Table I	- Instrumentation
Table II	- Bolometer Results
Table III (a)	- Photocell Results
Table III (b)	- Photocell Results
Table IV	- Photocell Results Temperatures Derived From Wien's Displacement Law
Table V	- Calorimeter Results
Table VI	- Radiant Energy From Explosions, 1961-1970

TABLE I  
INSTRUMENTATION

Instrument and Channel	Spectral Pass-band of System	Time Constant	Range from G.Z.	Field of View
<b>Bolometers</b>				
Silica	200 - 4,500 nm	300 $\mu$ s	1,700 m	20°
OY4 & Silica	510 - 2,700 nm			
OX2 & Silica	1,000 - 2,700 nm			
<b>Photocells</b>	Median      Effective Band-width	< 5 $\mu$ s	1,700 m	20°
1 (U.V.)	367 nm      3.22 nm			
2 (Blue)	442 nm      3.06 nm			
3 (Green)	512 nm      11.4 nm			
4 (Red)	624 nm      2.15 nm			
5 (I.R.)	759 nm      7.55 nm			
6 (I.R.)	936 nm      23.7 nm			
<b>Calorimeters</b>	Silica Window			
5 - 1	200 - 4,500 nm	11 s	1,700 m	80°
5 - 2	200 - 4,500 nm	11 s		
<b>Calorimeters</b>	Silica Window			
10 - 1	200 - 4,500 nm	18 s	600 m	80°
30 - 1	200 - 4,500 nm	40 s		
10 - 2	200 - 4,500 nm	18 s		
250 - 1	200 - 4,500 nm	75 s		

All instruments on a bearing of approximately 180° (south) from ground-zero.

TABLE II  
BOLOMETER RESULTS

Time t ms	Irradiance at Site H cal cm <sup>-2</sup> s <sup>-1</sup> × 10 <sup>-3</sup>			Ratio of Irradiances H <sub>OY4</sub> / H <sub>OX2</sub>	Distribution Temperature T <sub>D</sub> °K × 10 <sup>3</sup>	Transmission Factor a	Radiant Intensity J = Hr <sup>2</sup> /a cal ster <sup>-1</sup> s <sup>-1</sup> × 10 <sup>7</sup>
	Silica	OY4	OX2				Silica Band
1.0	25					0.90	80
1.1	40					0.90	128
1.2	48					0.90	154
1.25	49					0.90	157
1.3	48					0.90	154
1.4	43.5					0.90	140
1.5	39.0					0.90	125
2.0	24.5					0.89	80
2.5	21.5					0.87	71
3	20.5					0.86	69
4	19.5					0.82	69
5	19.8	16.3	8.2	1.99	3.7	0.78	74
7	20.2	17.0	9.9	1.72	3.3	0.74	79
10	20.7	18.0	12.0	1.5	2.85	0.68	87
12	21.3					0.66	93
15	22.2	18.6	13.9	1.34	2.55	0.64	100
20	23.5	19.4	15.4	1.26	2.40	0.63	108
25	24.0	19.9	16.5	1.21	2.25	0.62	112
30	23.7	19.9	17.0	1.17	2.15	0.61	112
40	22.5	22.5	16.9	1.14	2.10	0.60	108



TABLE II (cont'd)

Time t ms	Irradiance at Site H cal cm <sup>-2</sup> s <sup>-1</sup> × 10 <sup>-3</sup>			Ratio of Irradiances H <sub>OY4</sub> / H <sub>OX2</sub>	Distribution Temperature T <sub>D</sub> °K × 10 <sup>3</sup>	Transmission Factor a	Radiant Intensity J = Hr <sup>2</sup> /a cal ster <sup>-1</sup> s <sup>-1</sup> × 10 <sup>7</sup>
	Silica	OY4	OX2				Silica Band
50	21.0	18.1	16.3	1.11	1.95	0.60	101
70	18.2	15.8	14.5	1.09	1.95	0.59	89
100	15.5	13.5	12.5	1.08	1.95	0.58	78
120	13.6					0.58	68
150	11.8	10.7	9.9	1.08	1.95	0.58	59
170	11.0					0.58	55
200	10.4	10.4	8.8	1.05	1.90	0.58	52
230	9.9					0.58	49
250	10.5	9.1	8.6	1.05	1.9	0.58	52
270	11.0						55
300	12.4	10.7	10.0	1.07	1.9	0.58	62
325	13.3	11.6	10.7	1.08	1.95	0.58	66
350	13.1	11.4	10.5	1.08	1.95	0.58	65
400	12.3	10.8	10.0	1.08	1.95	0.58	61
500	10.8	9.7	9.4	1.05	1.9	0.58	54
700	10.2	9.2	8.7	1.06	1.9	0.58	51
1000	9.0	8.4	7.8	1.07	1.9	0.58	45
1200	8.6	7.6	7.4	1.03	1.8	0.58	43
1500	7.8	6.8	6.6	1.03	1.8	0.58	39
2000	6.8	5.7	5.6	1.02	1.7	0.58	34
3000	5.6	4.3	4.3	1.00	1.6	0.57	28
4000	5.4	4.2	4.2	1.00	1.6	0.57	27
5000	4.8					0.57	26
7000	2.5					0.57	13.5
10000	1.45	0.79	1.1			0.55	7.6
12000	1.25	0.56	0.65			0.55	6.6
15000	0.87					0.55	4.6

TABLE III (a)

## PHOTOCELL RESULTS

Time t ms	Irradiance at Site (Range, r = 1,700m) H cal cm <sup>-2</sup> s <sup>-1</sup> × 10 <sup>-4</sup>						Spectral Irradiance at Site H <sub>λ</sub> cal cm <sup>-2</sup> s <sup>-1</sup> nm <sup>-1</sup> × 10 <sup>-6</sup>						Distribution Temperature T <sub>D</sub> °K × 10 <sup>3</sup>	
	Channel number						Channel number						From Ratio	
	1	2	3	4	5	6	1	2	3	4	5	6	H <sub>2</sub> /H <sub>5</sub>	H <sub>3</sub> /H <sub>6</sub>
0.80	0	0	0	0	0	0	0	0	0	0	0	0	0	0
0.83	0.96	0.88	2.40	0.33	0.28	0.70	0.32	0.29	0.21	0.15	0.04	0.03	20	10
0.86	1.36	1.70	4.42	0.60	0.95	1.38	0.45	0.55	0.39	0.28	0.13	0.06	10	10
0.90	1.90	2.34	5.77	0.79	1.45	2.00	0.63	0.77	0.51	0.37	0.19	0.08	9	9
0.94	2.19	2.78	6.80	0.92	1.80	2.50	0.73	0.91	0.60	0.43	0.24	0.11	9	8.4
1.0	2.42	3.18	8.00	1.04	2.14	2.96	0.81	1.04	0.70	0.49	0.28	0.13	8.5	8.2
1.1	2.56	3.51	9.24	1.16	2.32	3.56	0.85	1.09	0.81	0.54	0.31	0.15	8.8	8.0
1.2	2.48	3.64	9.78	1.22	2.48	4.00	0.83	1.19	0.86	0.57	0.33	0.17	8.4	7.8
1.3	2.32	3.57	9.86	1.19	2.60	4.26	0.77	1.17	0.87	0.56	0.35	0.18	8.0	7.5
1.4	2.02	3.30	9.32	1.11	2.57	4.26	0.67	1.08	0.82	0.51	0.34	0.18	7.8	7.2
1.5	1.71	2.96	8.39	1.05	2.44	4.13	0.57	0.97	0.74	0.49	0.32	0.17	7.3	7.0
1.7	1.22	2.34	6.94	0.92	2.09	3.73	0.41	0.77	0.61	0.43	0.28	0.16	7.0	6.7
2.0	0.77	1.69	5.16	0.73	1.70	3.13	0.26	0.55	0.45	0.34	0.23	0.13	6.7	6.2
2.2	0.63	1.43	4.54	0.65	1.55	2.91	0.21	0.47	0.40	0.30	0.21	0.12	6.4	6.0
2.5	0.52	1.26	4.12	0.59	1.50	2.76	0.17	0.41	0.36	0.27	0.20	0.12	6.2	5.9
3.0	0.43	1.05	3.54	0.57	1.48	2.78	0.14	0.34	0.31	0.26	0.20	0.12	5.8	5.5
4.0	0.21	0.72	3.00	0.51	1.46	3.06	0.07	0.24	0.26	0.24	0.19	0.13	4.9	4.8
5.0	0.15	0.52	2.41	0.47	1.48	3.43	0.05	0.17	0.21	0.22	0.20	0.14	4.4	4.3
7.0	0.06	0.32	1.70	0.40	1.47	3.74	0.02	0.10	0.15	0.19	0.20	0.16	3.8	3.8
10.0	0.03	0.17	1.03	0.32	1.35	3.85	0.01	0.06	0.09	0.15	0.18	0.16	3.3	3.2

TABLE III (a) (cont'd)

Time t ms	Irradiance at Site (Range, r = 1,700m) H cal cm <sup>-2</sup> s <sup>-1</sup> × 10 <sup>-4</sup>						Spectral Irradiance at Site H <sub>λ</sub> cal cm <sup>-2</sup> s <sup>-1</sup> nm <sup>-1</sup> × 10 <sup>-6</sup>						Distribution Temperature T <sub>D</sub> °K × 10 <sup>3</sup>	
	Channel number						Channel number						From Ratio	
	1	2	3	4	5	6	1	2	3	4	5	6	H <sub>2</sub> /H <sub>5</sub>	H <sub>3</sub> /H <sub>6</sub>
12	0.025	0.12	0.89	0.30	1.30	3.92	.008	.039	.078	0.14	0.17	0.17	3.1	3.1
15	0.021	0.12	0.79	0.28	1.28	4.02	.007	.039	.070	0.13	0.17	0.17	3.1	3.0
20	0.012	0.09	0.62	0.25	1.25	4.13	.004	.029	.055	0.12	0.17	0.17	2.9	2.8
25	0.003	0.06	0.51	0.22	1.18	4.06	.001	.020	.045	0.11	0.16	0.17	2.7	2.7
30		0.05	0.39	0.18	1.09	3.89		.016	.034	0.09	0.15	0.16	2.6	2.6
40		0.03	0.26	0.13	0.88	3.32		.001	.023	.060	0.12	0.14	2.5	2.5
50		0.018	0.16	0.09	0.71	2.80		.001	.014	.041	0.10	0.12	2.5	2.4
70		0.011	0.09	0.06	0.49	2.03			.008	.026	0.07	0.09	2.3	2.2
100		0.008	0.04	0.03	0.34	1.44			.004	.014	0.05	0.07	2.3	2.0
120					0.28	1.19					0.04	0.05		
150					0.23	0.81					.031	.034		
200					0.20	0.76					.027	.032		
250					0.19	0.73					.025	.031		
300					0.25	0.95					.032	.040		
325					0.27	1.04					.036	.044		
350					0.24	0.97					.032	.041		
400					0.22	0.87					.029	.037		
500					0.19	0.74					.025	.031		
600					0.19	0.70					.025	.029		
700					0.18	0.67					.024	.028		
800					0.18	0.64					.024	.027		
1000					0.17	0.60					.023	.025		

TABLE III (b)  
PHOTOCELL RESULTS

Time t ms	Apparent Fireball Area A cm <sup>2</sup> x 10 <sup>6</sup>	Apparent Radiant Emittance						Emittance Temperature			
		$W_{app} = H\pi r^2/A$ cal cm <sup>2</sup> s <sup>-1</sup>						$T_E$ °K x 10 <sup>3</sup>			
		Channel number						Channel number			
		1	2	3	4	5	6	2	3	5	6
0.83	0.5	17.4	15.9	43.5	5.98	5.07	12.7	6.7	7.0	4.9	5.7
0.86	0.55	22.4	28.0	72.8	9.88	15.6	22.7	7.7	8.0	6.7	7.4
0.90	0.60	28.7	35.3	87.1	11.9	21.9	30.2	8.2	8.4	7.6	8.4
0.94	0.80	24.8	31.5	77.0	10.4	20.4	28.3	8.0	8.1	7.4	7.9
1.00	0.90	24.4	32.0	80.5	10.5	21.5	29.8	8.0	8.2	7.5	8.1
1.1	1.0	23.2	31.8	83.7	10.5	21.0	32.3	8.0	8.3	7.5	8.5
1.2	1.2	18.7	27.5	73.8	9.21	18.7	30.2	7.8	8.0	7.0	8.2
1.3	1.5	14.0	21.6	59.6	7.19	15.7	25.7	7.3	7.5	6.8	7.7
1.5	1.9	8.15	14.1	40.0	5.01	11.6	19.2	6.7	6.9	6.4	6.8
1.7	2.3	4.81	9.22	27.3	3.62	8.23	14.7	6.1	6.2	5.6	6.1
2.0	2.9	2.41	5.28	16.1	2.28	5.31	9.78	5.6	5.6	5.0	5.3
2.2	3.2	1.78	4.05	12.9	1.84	4.39	8.24	5.3	5.4	4.8	5.1
2.5	3.9	1.21	2.93	9.57	1.37	3.48	6.46	5.1	5.1	4.5	4.7
3.0	5.1	0.764	1.87	6.29	1.01	2.63	4.94	4.7	4.8	4.1	4.2
5.0	10.5	0.129	0.449	2.08	0.406	1.28	2.96	3.9	4.0	3.6	3.8
7	14.5	0.0375	0.200	1.06	0.250	0.918	2.34	3.5	3.6	3.4	3.6
10	22.5	0.0121	0.0685	0.415	0.129	0.544	1.55	3.1	3.2	3.1	3.2
15	37.5	0.00507	0.0290	0.191	0.0676	0.309	0.971	2.9	3.0	2.8	3.0
20	51.0	0.00213	0.0160	0.110	0.0444	0.222	0.734	2.8	2.8	2.7	2.8
25	65.0	0.000418	0.00836	0.0711	0.0307	0.164	0.566	2.6	2.7	2.6	2.7
30	78		0.00582	0.0453	0.0210	0.127	0.453	2.6	2.6	2.6	2.6
40	104		0.00262	0.0227	0.0113	0.0768	0.290	2.4	2.5	2.4	2.4
50	130		0.00126	0.0112	0.00622	0.0496	0.142	2.3	2.3	2.3	2.2
70	166		0.00060	0.00492	0.00306	0.0268	0.111	2.2	2.1	2.1	2.1
100	200		0.00036	0.00182	0.00136	0.0154	0.0654	2.1	2.0	2.0	2.0

TABLE IV

## PHOTOCELL RESULTS

TEMPERATURES DERIVED FROM WIEN'S DISPLACEMENT LAW

$$\lambda_{\max} \cdot T = \text{Constant} = 0.289 \text{ cm } ^\circ\text{K}$$

Time	Wavelength at maximum Irradiance	Temperature	Average Distribution Temperature (from Figure 5)
t	$\lambda_{\max}$	$T = \frac{0.289}{\lambda_{\max}} \times 10^4$	$T_D$
ms	nm	$^\circ\text{K} \times 10^3$	$^\circ\text{K} \times 10^3$
1.2	430	6.7	8.1
1.4	440	6.6	7.5
1.7	445	6.5	6.8
2.0	450	6.4	6.6
3.0	460	6.3	5.6
4.0	540	5.3	4.8
5.0	675	4.3	4.4
7.0	775	3.7	3.8
10.0	825	3.5	3.3

TABLE V  
CALORIMETER RESULTS

Calorimeter Number	Cooling Time-constant  s	Distance from Ground Zero  r m	Radiant Density  u cal cm <sup>-2</sup> × 10 <sup>-3</sup>	Radiant Energy  U cal × 10 <sup>10</sup>		
				0-4s	0-10s	0-20s
10-1	18	600	415	1.6	2.9	3.1
30-1	40	600	475	1.7	3.2	3.5
10-2	18	600	466	1.8	3.3	3.5
250-1	75	600	490	1.7	3.3	3.7
5-1	11	1,700	56.3	2.2	3.6	3.7
5-1	11	1,700	54.3	2.2	3.5	3.6

$$U = 4\pi r^2 \rho a^{-1}$$

where  $\rho = 1.06$ , a correction factor for the energy not transmitted by the silica windows.

At 600 m range,  $a^{-1} = 1.54$  (65% Transmission)

At 1,700 m range,  $a^{-1} = 1.73$  (58% Transmission)

TABLE VI  
RADIANT ENERGY FROM EXPLOSIONS, 1961-1970

Date	Weight of TNT	Shape of Charge	Range of Instruments	Type of Instruments	Radiant Energy	Percentage of Explosive Yield
	Ton		m		cal × 10 <sup>10</sup>	%
1961	100	Hemisphere	300 1,175	Calorimeters Bolometers	0.78 0.44	7.8 4.4
1962	20	Hemisphere	184 873	Calorimeters Bolometers	0.34 0.34	17 17
1962	5	Hemisphere	152	Calorimeters	0.075	15
1963	20	Hemisphere	185	Calorimeters	0.14	7.0
1963	5	Hemisphere	164	Calorimeters	0.032	6.1
1964	500	Hemisphere	600 1,825 1,825	Calorimeters Calorimeters Bolometers	2.7 2.8 2.9	5.4 5.6 5.8
1966	20	Sphere	1,000 1,000	Calorimeters Bolometers	0.53 0.54	26 27
1966	20-Ton TNT equiv. Hemisphere		250	Calorimeters	1.4	70
	Propane-Oxygen Mixture		1,000	Calorimeters	1.5	75
			1,000	Bolometers	1.6	80
1970	500	Sphere	600 1,700 1,700	Calorimeters Calorimeters Bolometers	3.5 3.7 3.7	7.0 7.4 7.4

1966, 20-Ton sphere was detonated on a tower 85 feet above ground level

1970, 500-Ton sphere was tangential to the ground

All hemi-spherical charges were detonated on the ground

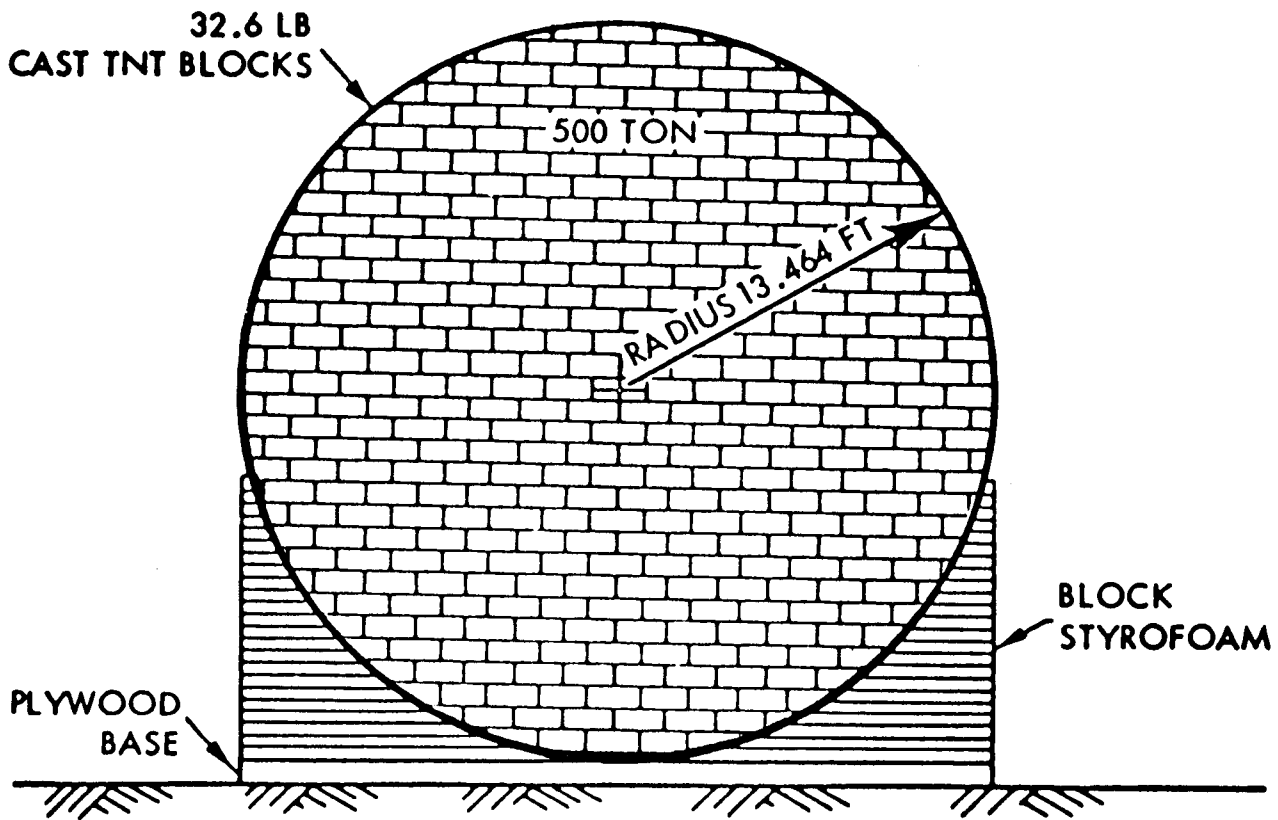
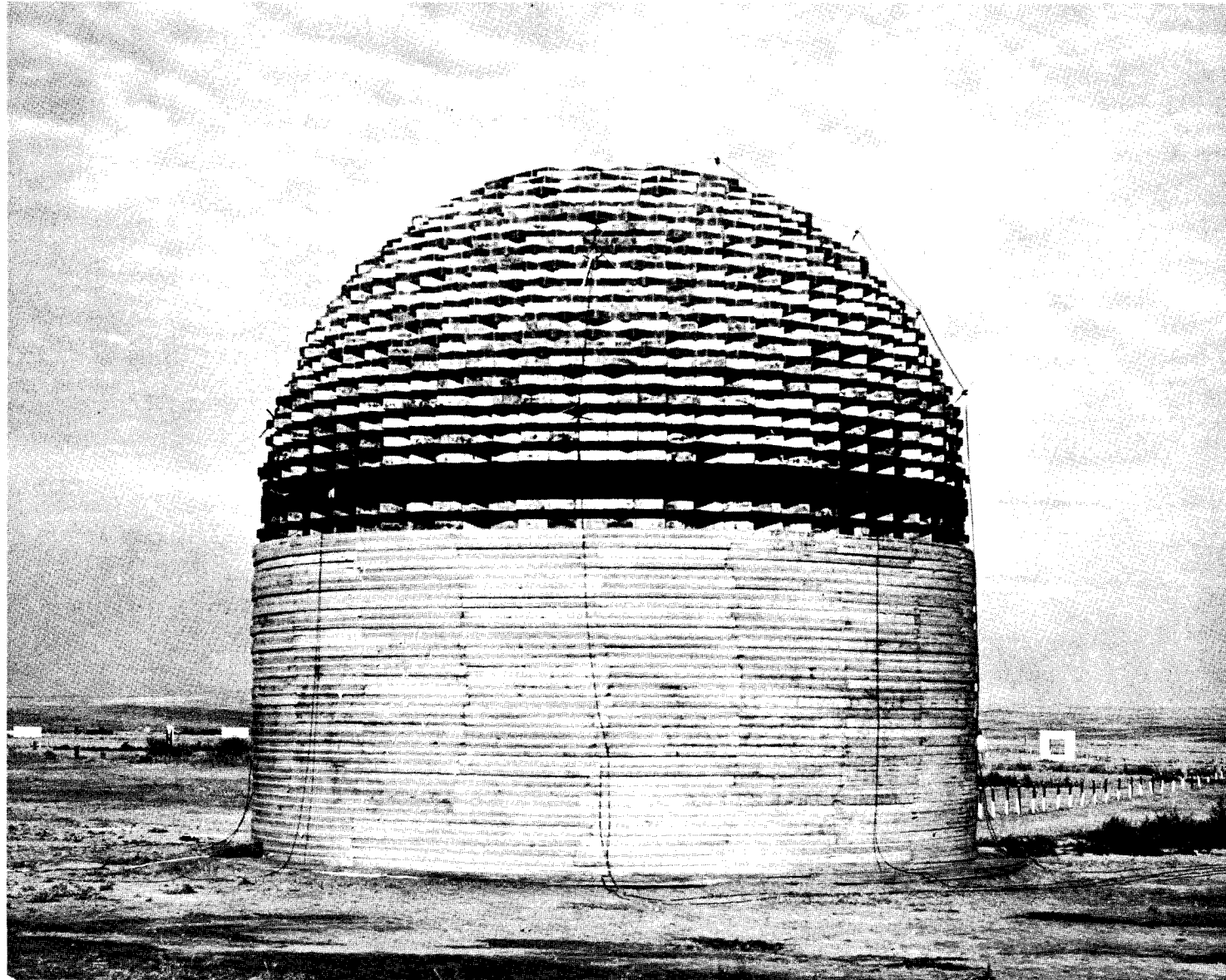


Fig. 1. Cross-section of charge and support.





*Fig. 2. 500 ton charge used for Prairie Flat.*

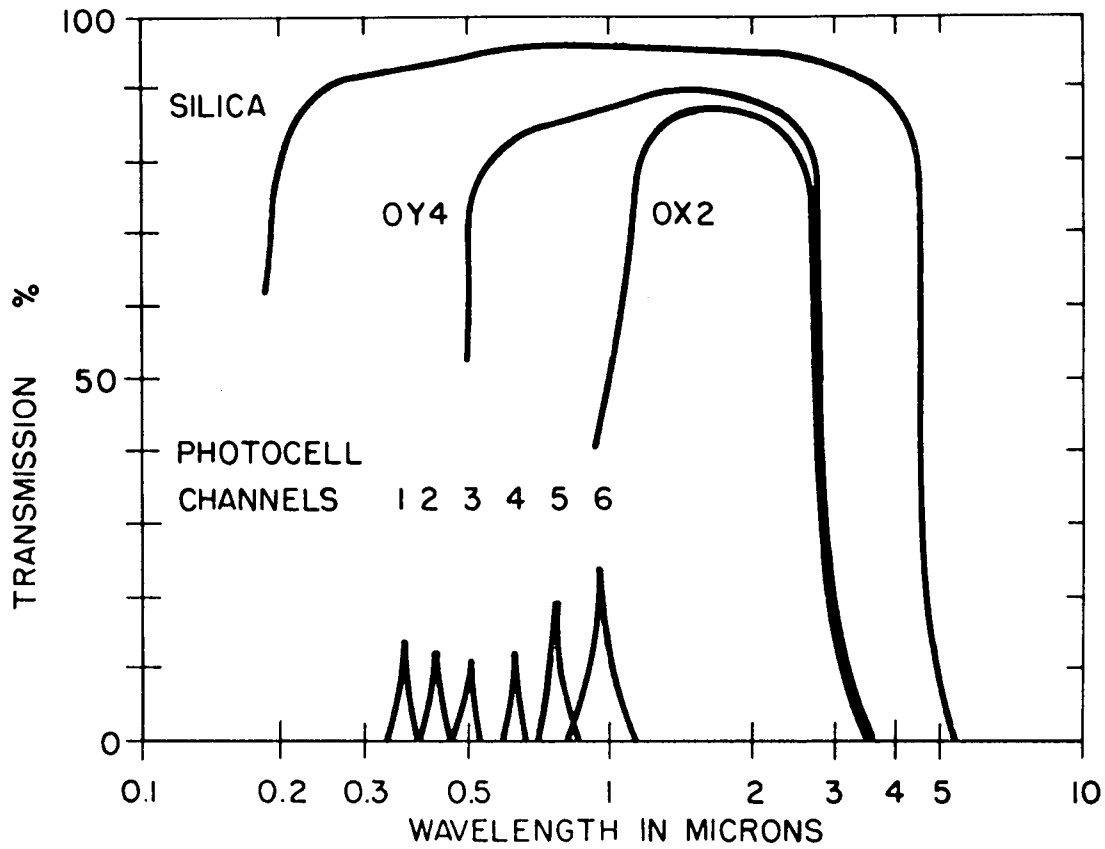


Fig. 3. Filter transmissions.

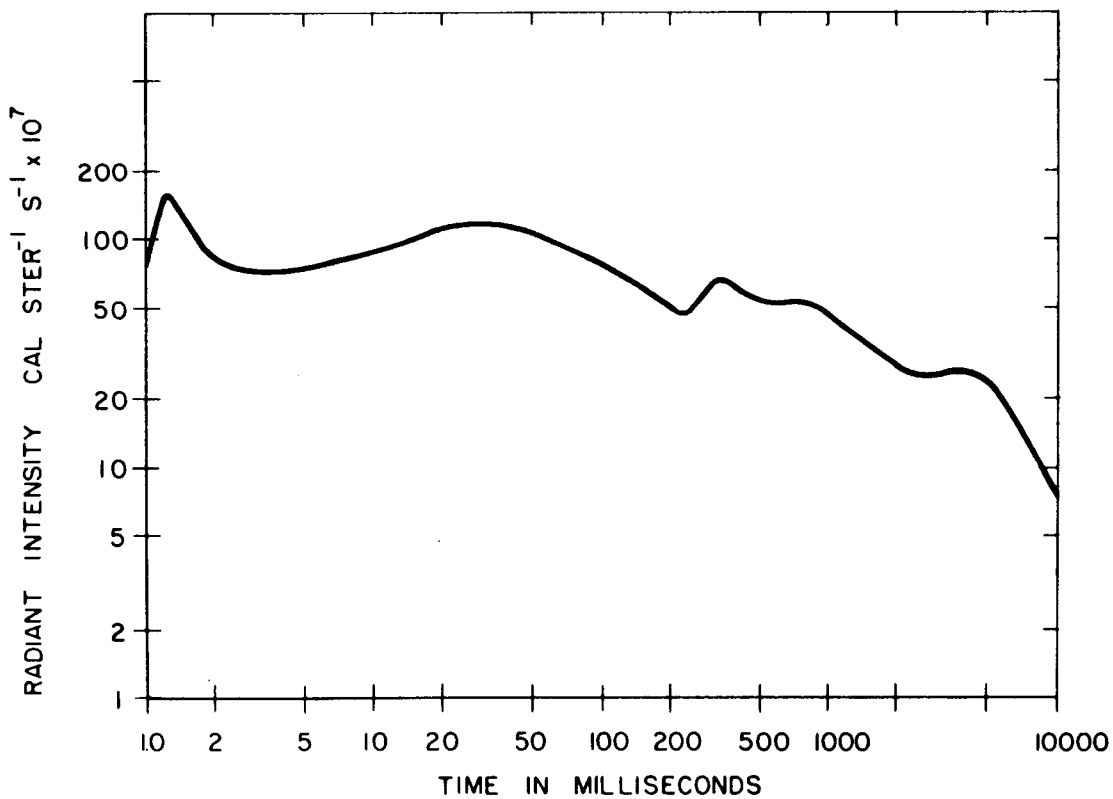


Fig. 4. Thermal pulse (from bolometer results, silica band).

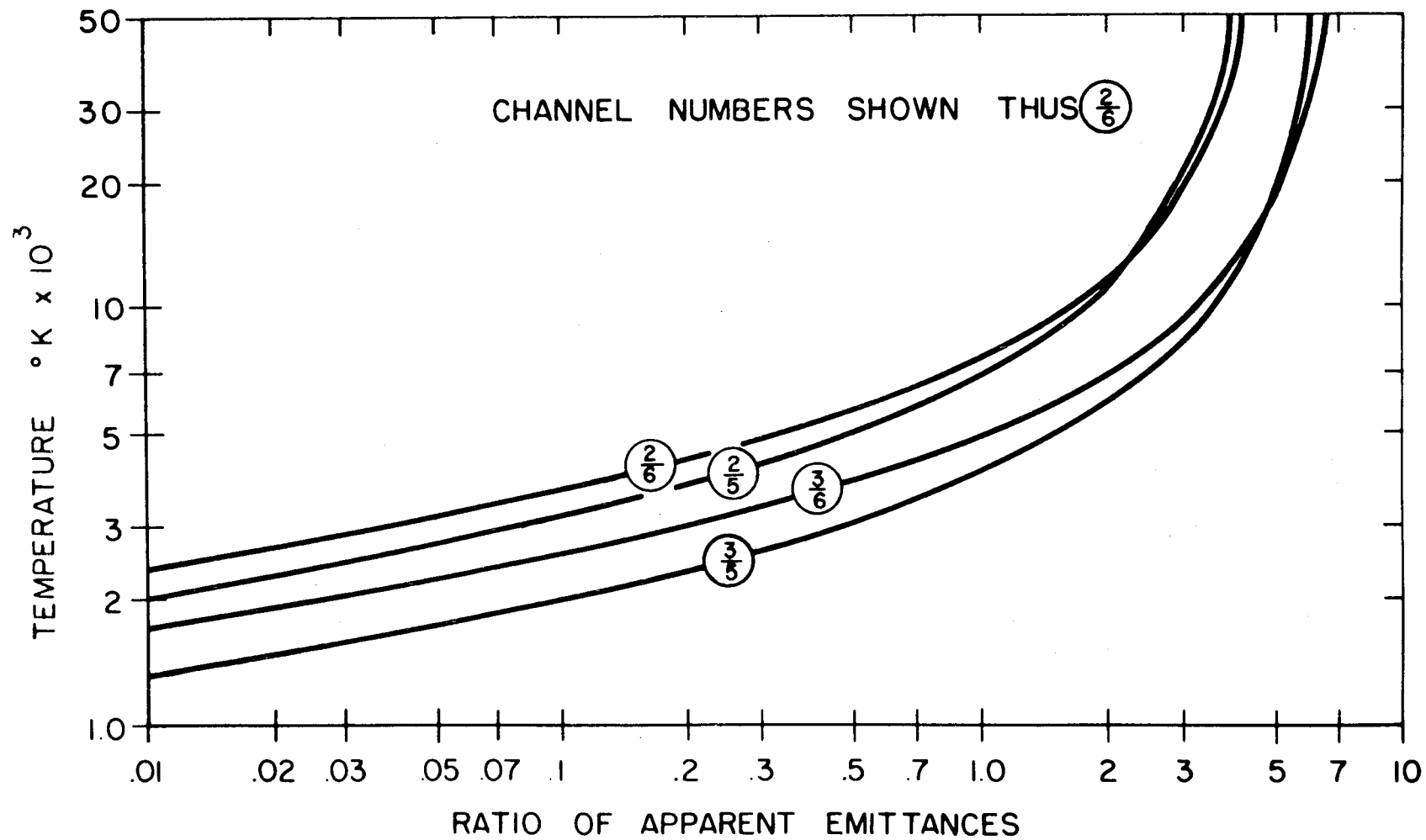


Fig. 5. Distribution-temperature calibration curves (photocell system).

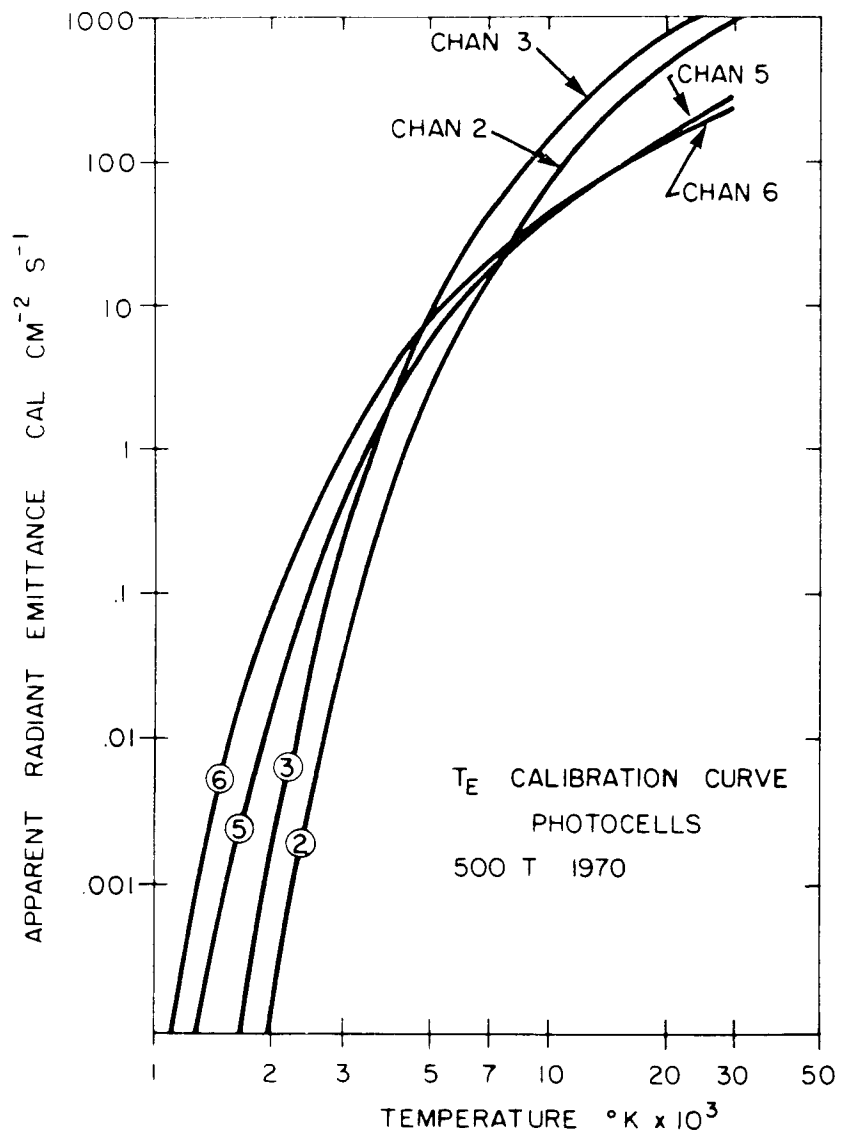


Fig. 6. Emittance-temperature calibration (photocells).

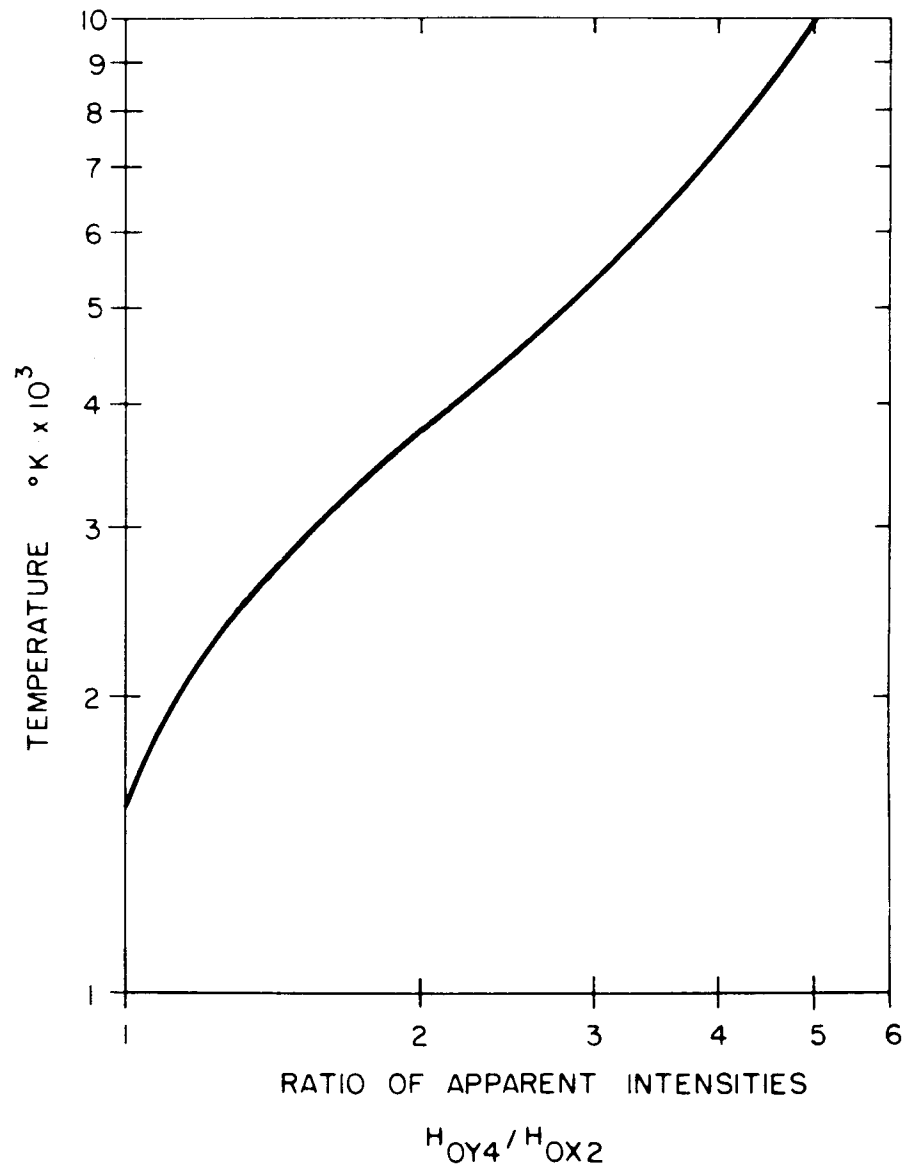


Fig. 7. Distribution-temperature calibration curve (bolometer system).

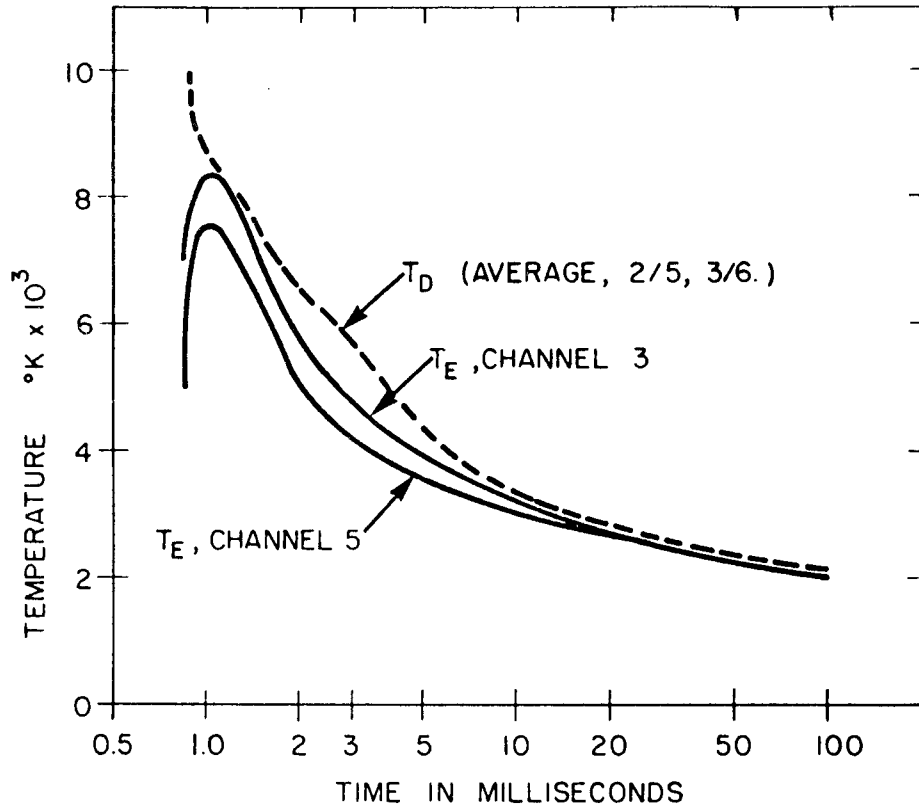


Fig. 8. Fireball temperature (from photocell results).

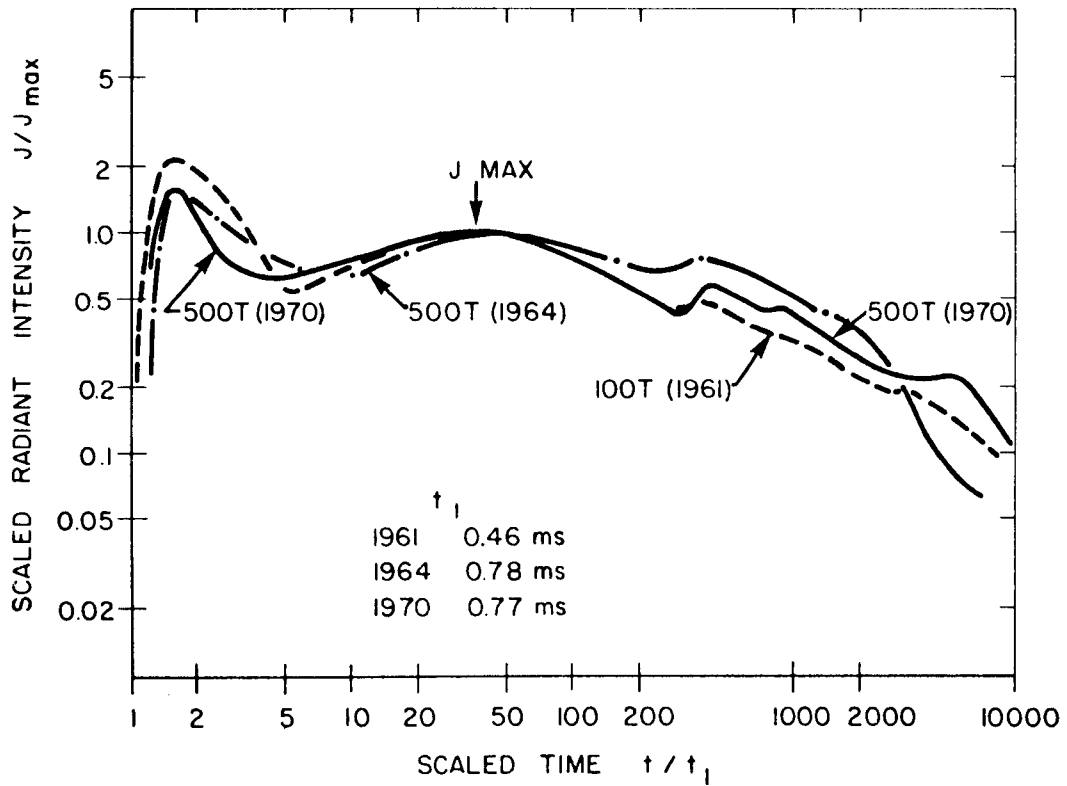


Fig. 9. Thermal pulses from T.N.T. explosions.

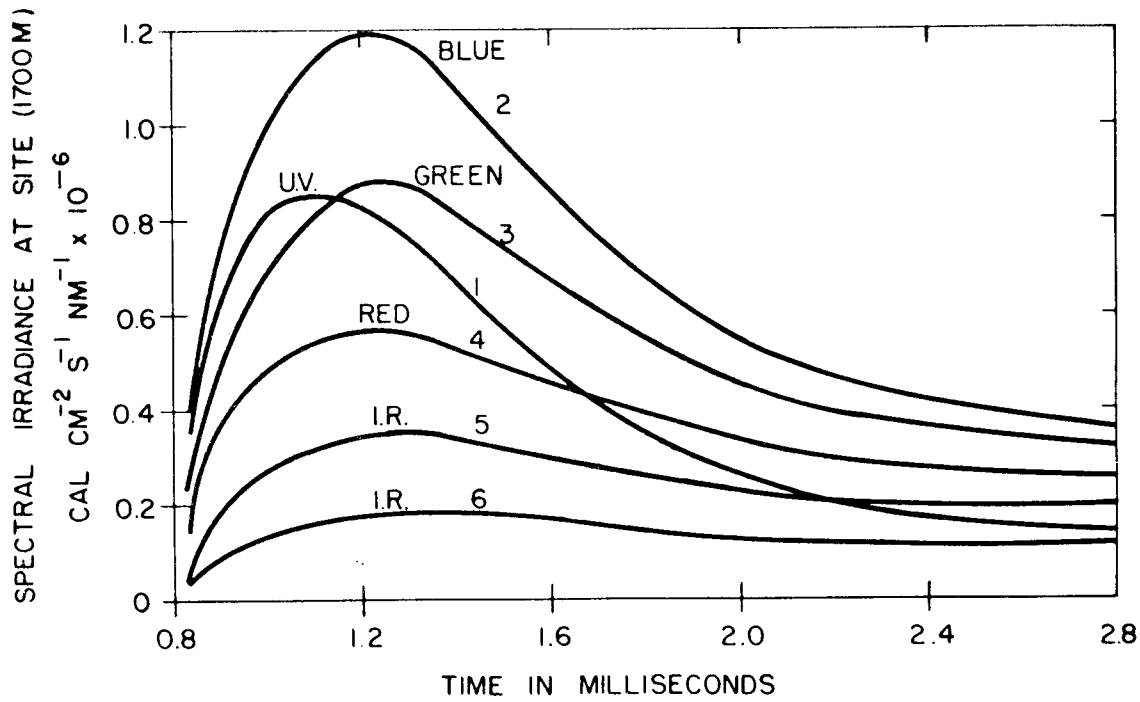


Fig. 10. Spectral distribution at early times (photocell results).

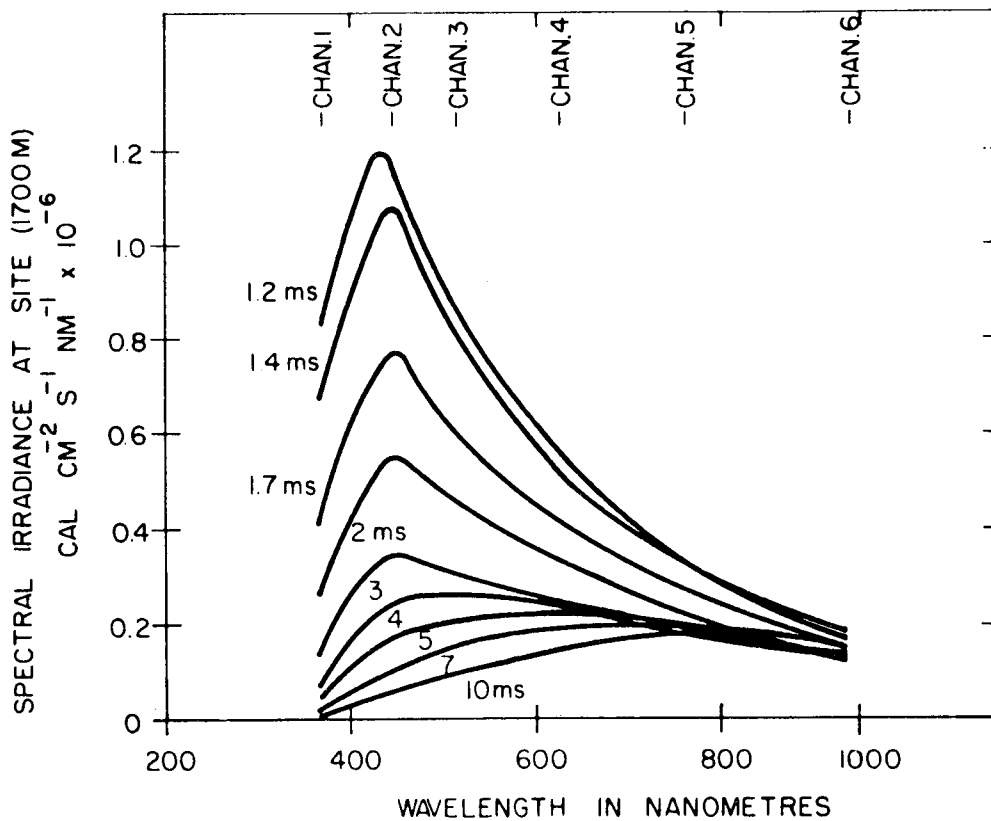
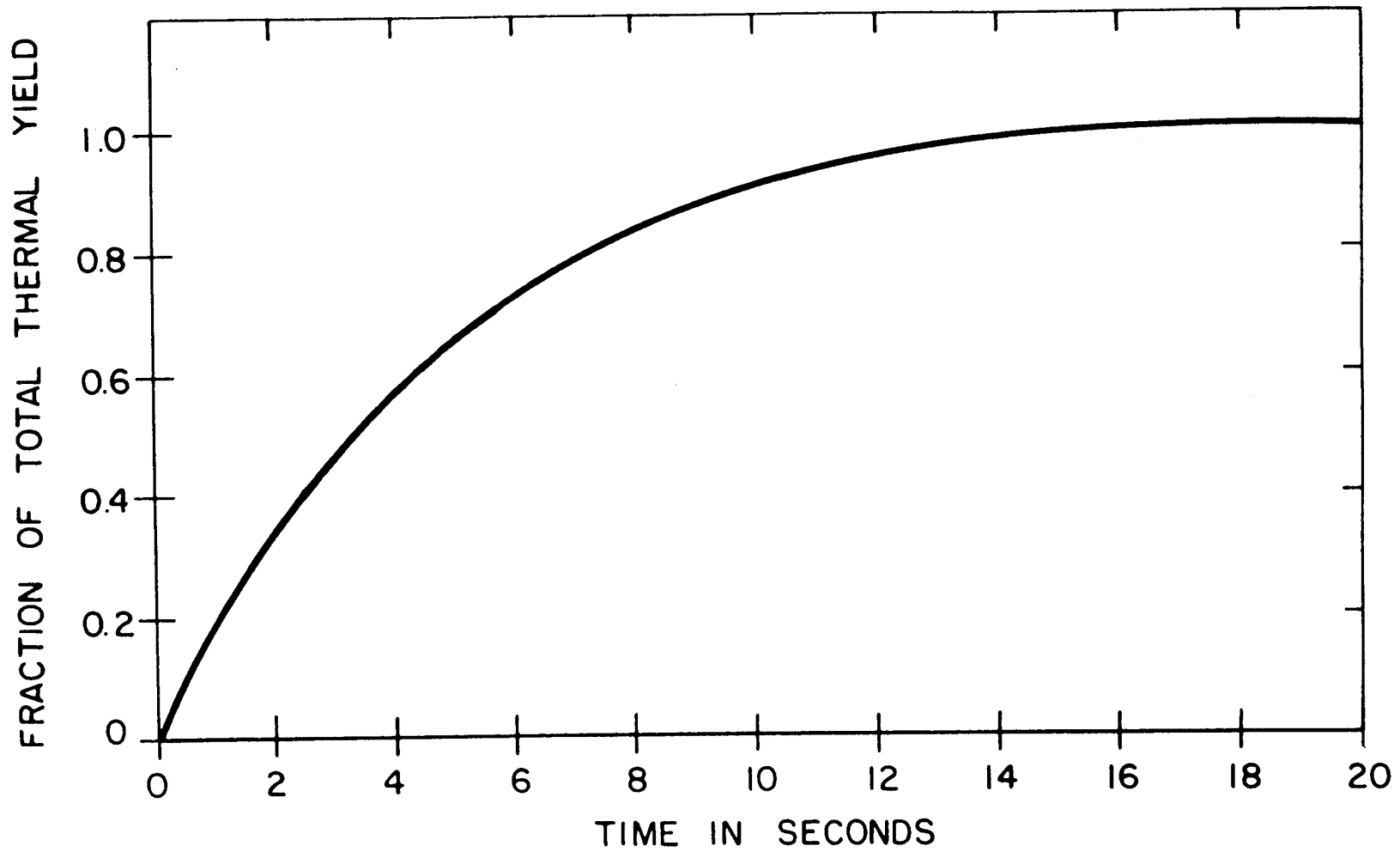


Fig. 11. Spectral distribution at early times (photocell results).



*Fig. 12. History of thermal yield.*

V

0201 DREC

(NON-CONTROLLED GOODS)  
DMC A  
REVIEW: GCEC December 2012

414

0202 404576

0203 642

UNCLASSIFIED

Security Classification

0204a DOCUMENT CONTROL DATA - R & D (Security classification of title, body of abstract and indexing annotation must be entered when the overall document is classified)		
1. ORIGINATING ACTIVITY Defence Research Establishment Ottawa, <del>Defence Research Board, Ottawa, Ontario KIA 0Z</del>		2a. DOCUMENT SECURITY CLASSIFICATION UNCLASSIFIED
		2b. GROUP OINT (CAN)
3. DOCUMENT TITLE 04a OPERATION DIAL PACK 1970 - CANADIAN PROJECT A7 - THERMAL RADIATION MEASUREMENTS (U)		
4. DESCRIPTIVE NOTES (Type of report and inclusive dates) <del>DREC Report 642</del>		
5. AUTHOR(S) (Last name, first name, middle initial) 1101 Pattman, J.D.R.		
6. DOCUMENT DATE 46 August 1971	7a. TOTAL NO. OF PAGES 0901 3024	7b. NO. OF REFS 0902 12
8a. PROJECT OR GRANT NO. 35 D-16-01-39	9a. ORIGINATOR'S DOCUMENT NUMBER(S)	
8b. CONTRACT NO.	9b. OTHER DOCUMENT NO.(S) (Any other numbers that may be assigned this document)	
10. DISTRIBUTION STATEMENT		
11. SUPPLEMENTARY NOTES		12. SPONSORING ACTIVITY
13. ABSTRACT Thermal radiation from the DIAL PACK 500-ton TNT explosion was recorded in selected wavelength bands, using a high-speed bolometer system, photo-electric detectors, and calorimeters. The radiation was received in both broad and narrow spectral bands, defined by placing suitable combinations of glass filters and silica windows in front of the detectors. Results were obtained from all instruments used, and are presented in this report. These include measurements of the total thermal energy radiated, the thermal pulse shape as shown by records of irradiance versus time, and the variation of spectral distribution as a function of time. Estimation of the apparent temperature of the fireball surface is also discussed. Some comparisons are made with results from previous large TNT explosions.		

ml



## KEY WORDS

DIAL PACK

Blast Trials

Thermal Radiation

Spectra of Fireball Radiation

## INSTRUCTIONS

1. **ORIGINATING ACTIVITY:** Enter the name and address of the organization issuing the document.
- 2a. **DOCUMENT SECURITY CLASSIFICATION:** Enter the overall security classification of the document including special warning terms whenever applicable.
- 2b. **GROUP:** Enter security reclassification group number. The three groups are defined in Appendix 'M' of the DRB Security Regulations.
3. **DOCUMENT TITLE:** Enter the complete document title in all capital letters. Titles in all cases should be unclassified. If a sufficiently descriptive title cannot be selected without classification, show title classification with the usual one-capital-letter abbreviation in parentheses immediately following the title.
4. **DESCRIPTIVE NOTES:** Enter the category of document, e.g. technical report, technical note or technical letter. If appropriate, enter the type of document, e.g. interim, progress, summary, annual or final. Give the inclusive dates when a specific reporting period is covered.
5. **AUTHOR(S):** Enter the name(s) of author(s) as shown on or in the document. Enter last name, first name, middle initial. If military, show rank. The name of the principal author is an absolute minimum requirement.
6. **DOCUMENT DATE:** Enter the date (month, year) of Establishment approval for publication of the document.
- 7a. **TOTAL NUMBER OF PAGES:** The total page count should follow normal pagination procedures, i.e., enter the number of pages containing information.
- 7b. **NUMBER OF REFERENCES:** Enter the total number of references cited in the document.
- 8a. **PROJECT OR GRANT NUMBER:** If appropriate, enter the applicable research and development project or grant number under which the document was written.
- 8b. **CONTRACT NUMBER:** If appropriate, enter the applicable number under which the document was written.
- 9a. **ORIGINATOR'S DOCUMENT NUMBER(S):** Enter the official document number by which the document will be identified and controlled by the originating activity. This number must be unique to this document.
- 9b. **OTHER DOCUMENT NUMBER(S):** If the document has been assigned any other document numbers (either by the originator or by the sponsor), also enter this number(s).
10. **DISTRIBUTION STATEMENT:** Enter any limitations on further dissemination of the document, other than those imposed by security classification, using standard statements such as:
  - (1) "Qualified requesters may obtain copies of this document from their defence documentation center."
  - (2) "Announcement and dissemination of this document is not authorized without prior approval from originating activity."
11. **SUPPLEMENTARY NOTES:** Use for additional explanatory notes.
12. **SPONSORING ACTIVITY:** Enter the name of the departmental project office or laboratory sponsoring the research and development. Include address.
13. **ABSTRACT:** Enter an abstract giving a brief and factual summary of the document, even though it may also appear elsewhere in the body of the document itself. It is highly desirable that the abstract of classified documents be unclassified. Each paragraph of the abstract shall end with an indication of the security classification of the information in the paragraph (unless the document itself is unclassified) represented as (TS), (S), (C), (R), or (U).  
  
The length of the abstract should be limited to 20 single-spaced standard typewritten lines; 7½ inches long.
14. **KEY WORDS:** Key words are technically meaningful terms or short phrases that characterize a document and could be helpful in cataloging the document. Key words should be selected so that no security classification is required. Identifiers, such as equipment model designation, trade name, military project code name, geographic location, may be used as key words but will be followed by an indication of technical context.